Published in final edited form as:

Nature. 2012 August 9; 488(7410): 218–221. doi:10.1038/nature11239.

Human Dorsal Anterior Cingulate Cortex Neurons Mediate Ongoing Behavioral Adaptation

Sameer A. Sheth[*,1], **Matthew K. Mian**[*,1], **Shaun R. Patel**[1,2], **Wael F. Asaad**[3], **Ziv M. Williams**[1], **Darin D. Dougherty**[4], **George Bush**[4], and **Emad N. Eskandar**[1]

[1]Nayef Al-Rodhan Laboratories, Department of Neurosurgery, Massachusetts General Hospital, Boston, MA

[2]Department of Anatomy and Neurobiology, Boston University School of Medicine, Boston, MA

[3]Department of Neurosurgery, Alpert Medical School, Brown University and Rhode Island Hospital, Providence, RI

[4]Department of Psychiatry, Massachusetts General Hospital, Boston, MA

Abstract

The ability to optimize behavioral performance when confronted with continuously evolving environmental demands is a key element of human cognition. The dorsal anterior cingulate cortex (dACC), which lies on the medial surface of the frontal lobes, plays an important role in regulating cognitive control. Hypotheses regarding its function include guiding reward-based decision making[1], monitoring for conflict between competing responses[2], and predicting task difficulty[3]. Precise mechanisms of dACC function remain unknown, however, due to the limited number of human neurophysiological studies. Here we demonstrate with functional imaging and human single-neuron recordings that the firing of individual dACC neurons encodes current and recent cognitive load. We show that the modulation of current dACC activity by previous activity produces a behavioral adaptation that accelerates reactions to cues of similar difficulty as previous ones, and retards reactions to cues of differing difficulty. Furthermore, this conflict adaptation, or Gratton effect[2,4], is abolished after surgically targeted dACC ablation. Our results demonstrate that the dACC provides a continuously updated prediction of expected cognitive demand to optimize future behavioral responses. In situations with stable cognitive demands, this signal promotes efficiency by hastening responses, but in situations with changing demands, it engenders accuracy by delaying responses.

Correspondence and request for materials should be addressed to ENE (eeskandar@partners.org)..

*These authors contributed equally to this work.

Supplementary Information is linked to the online version of the paper at www.nature.com/nature

Author Contributions ENE, WFA, ZMW, and DDD designed the study. GB administered and interpreted the fMRI scans. ENE performed the surgical procedures, and SAS, MKM, SRP, and WFA obtained the neuronal recordings. SAS and MKM analyzed the data and wrote the manuscript. All authors edited the manuscript.

Author Information Reprints and permissions information is available at www.nature.com/reprints.

The authors declare no competing financial interests.

There are no conflicts of interest.

Human cognition is characterized by the ability to parse and evaluate a stream of constantly changing environmental stimuli in order to choose the most appropriate response in evolving conditions. The dorsal anterior cingulate cortex (dACC) is thought to play an important role in regulating cognitive control over goal-directed behavior. Various theories postulate its involvement in linking reward-related information to action[1,5,6], monitoring for conflict between competing responses[2,7,8], or detecting the likelihood of error commission[3,9,10]. Despite substantial information from functional magnetic resonance imaging (fMRI), event-related potential, and lesion studies, considerable debate continues to exist regarding the neurophysiological basis of its regulatory role.

We studied dACC function using a combination of fMRI, single-neuronal recordings, and with pre- and post-lesion behavior in human subjects undergoing surgical cingulotomy—a procedure in which a precise stereotactically targeted lesion is created in the dACC. Microelectrode recordings, which are routinely performed during the procedure[1,11,12], allowed us to record from individual dACC neurons. Six subjects participated, and in four of these we also obtained a preoperative fMRI using the same task. In four we recorded behavioral responses using the same task immediately following cingulotomy.

Subjects performed the multi-source interference task (MSIT)[13], a Stroop-like task in which they viewed a cue consisting of three numbers and had to indicate via button-press the unique number (‘target’) that differed from the other two numbers (‘distracters’) (Figure 1A). By varying the position of the target and the identity of the distracters, the task established four distinct trial types (Figure 1B), which were presented to the subject randomly. These trial types contained three levels (Type 0, 1, and 2 trials; Figure 1B) of *cognitive interference*, operationally defined here as the tendency of an irrelevant stimulus feature (*e.g.*, position of the target) to impede simultaneous processing of the relevant stimulus feature (*e.g.*, identity of the target).

When comparing high-interference (Type 2) to non-interference (Type 0) trials, there was increased fMRI signal within the dACC (Figure 1D), indicating increased neuronal population activity during trials with greater cognitive interference. Other cortical regions known be involved in this decision-making network, such as the dorsolateral pre-frontal cortex (DLPFC), were similarly activated to a greater degree in the high interference condition (Figure S1). The spatial distribution and magnitude of these changes were similar to those previously observed in healthy volunteers[14,15], suggesting that this function is spared in the dACC in our subject population and comparable to normal subjects. We co-registered the postoperative MRI (Figure 1E) with the preoperative fMRI, confirming that the recording and lesion site co-localized with the region of fMRI activation.

During intraoperative microelectrode recordings, subjects performed the task accurately, with an error rate of 1.4%. Reaction times (RTs) were modulated by degree of interference in a dose-dependent fashion (Figure 1C, S2; $p < 1 \times 10^{-20}$, ANOVA). The trial type-dependent reaction times and low error rates were consistent with the tendency to sacrifice speed for accuracy that is often observed in Stroop-like tasks[8,16].

We recorded 59 well-isolated, single dACC neurons, with an average baseline firing rate of 5.7 ± 0.7 (mean ± s.e.m.) spikes/sec. We identified three distinct sub-populations of neurons based on their maximal task-responsiveness: those firing preferentially (1) before the cue (n = 12; 20%); (2) after presentation of the cue (n = 24; 41%); and (3) after the behavioral choice (n = 23; 39%). The largest group, or cue-responsive neurons, showed distinct modulation of firing based on the degree of interference present in the cue (p = 0.02, ANOVA, Table S1). Paralleling the pattern for RTs, firing rates for Type 2 trials were higher than those for Type 1 trials, which were higher than those for Type 0 trials. This effect during the cue epoch was observable at the level of individual neurons (Figure 2A, B), as well as at the cue neuron population level (Figure 2C, D). Inclusion of the entire recorded neuronal population produced similar effects (Figure S3), and using raw rather than normalized rates did not change this result. Neuronal activity within the dACC thus correlated with the degree of cognitive interference present in the cue.

The trial type-dependent modulation in firing rate could either be a consequence of dACC neuron sensitivity to the amount of conflict engendered by the cue[2,17] or to the number of potential responses activated by the cue[18] (Supplementary Note 1). To distinguish between these possibilities, we identified trials in which the number of potential responses remained constant (two), but the amount of conflict varied (one or two types of conflict). Firing rates were significantly higher ($p = 6.4 \times 10^{-3}$, Mann-Whitney test) in higher conflict trials, indicating that dACC neurons were encoding conflict *per se*, and not the potential number of responses (Figure S4). Reaction times for the higher conflict trials were also significantly higher ($p = 1.5 \times 10^{-4}$, t-test), providing behavioral evidence for the increase in perceived conflict. In a two-way ANOVA (with degree of conflict as one variable and the number of possible responses as the other variable) including all trials, the degree of conflict was a significant independent predictor of firing rate ($p = 5.7 \times 10^{-3}$), whereas the number of possible responses was not (p = 0.11).

Current models of dACC function, whether predicated upon conflict monitoring[2,8,17], reinforcement learning[3,19], or reward-based decision making[1,20,21], require that future dACC activity reflects past experience, but modulation of dACC firing based on recent history has not been demonstrated at the single-neuronal level. To determine whether dACC neuronal firing rates are influenced by previous activity, we separated Type 0 and Type 2 trials based on whether they were immediately preceded by a trial containing interference (Type 1 or 2) or not (Type 0). In both cases, dACC neuronal activity increased more rapidly following the cue when the preceding trial contained interference (Figure 3A, B). Average magnitude of the cue neuron signal was greater in trials preceded by interference. This finding held for the entire neuronal population as well (Figure S5), and was not altered by using raw rather than normalized rates.

The association between previous and current trial activity was maintained across all successive trial pairs. On a trial-by-trial basis including all trial types, previous trial activity during the cue period significantly correlated with current trial activity (r = 0.15, $p = 2.0\times10^{-11}$ for cue neurons; r = 0.12, $p = 3.3\times10^{-16}$ for all neurons, Supplementary Note 2), demonstrating that dACC neurons encode information about both the current task context

and the recent past. This neural-neural correlation was not simply an effect of drift in the recordings (Supplementary Note 3).

The behavioral correlate of this neuronal pattern of activity depended upon the identity of the current trial. Reaction times for Type 0 trials correlated positively with previous trial activity ($r = 0.13$, $p = 9.2\times10^{-3}$), meaning that preceding elevated activity (consistent with a previous difficult trial) predicted a longer RT on the current non-interference trial. Reaction times during Type 2 trials, however, correlated negatively with previous trial activity ($r = -0.09$, $p = 8.4\times10^{-3}$), meaning that preceding elevated activity predicted a shorter RT on the current interference trial. Taken together, these findings would predict that RTs for a particular trial type would be shorter when the preceding trial was of the same type, and longer when of a different type (Supplementary Note 4).

The behavioral responses bore out these predictions. Reaction times during noninterference trials were shorter when preceded by another non-interference trial (0→0) vs. an interference (1,2→0) trial (Figure 3C, S6A). Conversely, RTs during high interference trials were shorter when preceded by an interference (1,2→2) trial vs. a noninterference (0→2) trial (Figure 3D, S6B). This history-dependence of dACC neuronal activity provides a neurophysiological basis for the current data and previous observations of behavioral adaptations, known as micro-adjustments, conflict adaptation, or the Gratton effect[2,4,8,17,22,23].

We analyzed post-cingulotomy task performance, and thereby captured the acute behavioral manifestations of a precise, stereotyped, reproducible lesion to the previously recorded area (Figure S7). Error rate following cingulotomy was 1.3%, indicating that subjects had not changed in their ability to perform the task. The post-cingulotomy reaction time distribution was similar to that observed prior to the lesion (Figure 4A, S8A), with longer RTs associated with increasing interference ($p < 1 \times 10^{-12}$, ANOVA). Furthermore, there was no difference in pre- vs. post-cingulotomy mean RT ($p = 0.76$, t-test). Thus the dACC lesion did not significantly disrupt the subjects' ability to perform the task, nor did it affect the dependence of RT on the cognitive load presented by the current stimulus.

Strikingly, cingulotomy caused abolition of the history-dependent modulation of reaction times. The pre-lesion trial-to-trial adaptations in RT were significantly reduced after cingulotomy for both non-interference ($p = 2.2 \times 10^{-8}$, bootstrap test) and high-interference trials ($p = 7.1 \times 10^{-3}$). Consistently, the difference in RT attributable to the previous trial that existed before the lesion (Figure 3C, D, S6A, B) disappeared after the lesion (Figure 4B, C, S8B, C); that is, reaction times did not depend upon the preceding trial type. This effect was observable at the population level and at the level of individual subjects (Figure S9). Thus, although dACC lesions did not globally degrade subject performance, they eliminated the dependency of behavioral responses on recent experience.

These trial-to-trial behavioral adjustments (faster RT when the preceding trial type was the same as the current) are concordant with those reported by others[2,4,8,17,22,23]. During high interference trials preceded by a high interference trial, however, we observed increased dACC single neuron activity, whereas others have reported decreased BOLD fMRI

signal[2,17]. This apparent discrepancy may be explained by the fact that the peak fMRI signal (which occurs 5-7 seconds after the cue) reflects input synaptic activity evoked by both the appearance of the cue and evaluation of the response (which all occur within the first second after the cue). On the other hand, we recorded output spiking activity occurring within 500-750 ms after the cue. These complementary measures may thus reflect the spatiotemporal dynamics of conflict processing in the dACC.

In this task, increasing interference within the cue could variably be interpreted as representing increasing conflict between competing potential responses[8], likelihood of error commission[3], or energetic decision-making cost[20]. Consistent with these theories, we find that dACC activity correlates with these manifestations of cognitive demand. However, though the dACC is modulated by the cognitive load within the current task context, its function is not essential for generating the load-dependent behavioral response[16,24], as interference-dependent behavior was not altered following dACC ablation. In contrast, an intact dACC is required for trial-to-trial behavioral adjustments.

Previous studies have proposed that the dACC monitors for conflict between competing responses[7,8] and drives behavior towards efficient strategies[20]. Whereas previous human fMRI[2,17], ERP[25], and lesion[26] studies have implicated the dACC in this function, single unit data supporting this theory have been lacking. Moreover, non-human primate single unit recordings[18,21] and lesion[24] studies have arrived at opposite conclusions and cast doubt on the conflict monitoring theory[27]. We reconcile these issues by demonstrating fMRI and single neuronal conflict signals in the human dACC, as well as behavioral adjustments that disappear after a precisely targeted lesion. Our results support the view that the dACC is specifically responsible for providing a continuously updated account of predicted demand on cognitive resources. This account is particularly sensitive to relative shifts in situational complexity from instance to instance, weighted by the recent past. The salient influence of current dACC activity on future neuronal activity and behavior permits implementation of behavioral adjustments that optimize performance. In situations in which cognitive demands remain constant, this signal facilitates efficiency by accelerating responses. In situations involving rapidly changing demands, it promotes accuracy by retarding responses.

Methods Summary

Six subjects (4 male, age 37.5 ± 5 years) undergoing stereotactic cingulotomy for treatment-refractory obsessive-compulsive disorder provided informed consent and enrolled. The study was approved by our Institutional Review Board. The surgical procedure produces a stereotypical lesion with an average volume of 3.58 ± 1.24 cm^3, centered 9 mm lateral to midline, 18 mm anterior to the anterior commissure, and 30 mm superior to the AC-PC plane[28].

During surgery, subjects performed the Multi-Source Interference Task[13,14], which was presented on a computer monitor using a customized software package in MATLAB (MathWorks, Natick, MA)[29]. Each trial contained a stimulus consisting of three integers ranging from zero to three. One number (the unique “target”) differed from a pair of

"distracter" numbers. Subjects were asked to report, via button-press, the *identity* (rather than position) of the target (left button for "1", middle for "2", right for "3").

Functional MRI data were analyzed using Brain Voyager software (Brain Innovation, Maastricht, the Netherlands). Anatomical and functional data were co-registered and transformed into common Talairach space. A general linear model was constructed using predictors modeled by convolution with a standard hemodynamic response function. Single subject repeated-measures ANOVAs were performed on a voxel-wise basis. Multiple comparisons were accounted for by using a cluster constraint with regional false positive probability $p < 10^{-4}$, requiring a cluster of ≥7 contiguous voxels with $p < 0.05$.

For microelectrode recordings, an array of three tungsten microelectrodes (500-1500 kΩ; FHC, Bowdoin, ME) was attached to a motorized microdrive (Alpha Omega Engineering, Nazareth, Israel). Upon reaching the cingulate cortex, microelectrodes were held in place and monitored for approximately five minutes to assess signal stability. Putative neurons were not screened for task-responsiveness. Analog data were amplified, band-pass filtered between 300 Hz and 6 kHz, sampled at 20 kHz, and spike-sorted (Offline Sorter, Plexon, Dallas, TX).

Methods

Subjects

We enrolled 6 study subjects (4 male, mean ± s.e.m. age 37.5 ± 5 years) undergoing stereotactic cingulotomy for treatment-refractory obsessive-compulsive disorder (OCD). Evaluation for surgical candidacy was conducted by a multidisciplinary team consisting of psychiatrists, neurologists, and neurosurgeons. Subjects enrolled voluntarily, providing informed consent under a protocol approved by the Massachusetts General Hospital Institutional Review Board. The surgical procedure produces a stereotypical lesion with an average volume of 3.58 ± 1.24 (mean ± s.d.) cm^3, centered 9 mm lateral to midline, 18 mm anterior to the anterior commissure, and 30 mm superior to the AC-PC plane[28]. Subject participation was in no way related to clinical decision-making regarding their candidacy for surgery.

Behavioral Task

During the microelectrode recording portion of surgery, subjects performed the Multi-Source Interference Task (MSIT) (Figure 1A, B)[13,14]. The task was presented on a computer monitor using a customized software package in MATLAB (MathWorks, Inc., Natick, MA)[29]. Each trial contained a stimulus consisting of three integers ranging from zero to three. One number (the unique "target") differed from a pair of "distracter" numbers (*e.g.* 100, 323, etc.). Subjects were asked to report, via button-press, the *identity* (rather than the position) of the target (left button for "1", middle for "2", right for "3").

Functional MRI

Functional MRI was performed prior to surgery using a 3.0 T scanner (Allegra; Siemens AG, Munich, Germany) and head coil. The MSIT task was presented on a screen visible via

a tilted mirror, and controlled using MacStim 2.6 software (WhiteAnt Occasional Publishing, West Melbourne, Australia). Scans were acquired with the following specifications: 15 coronal sections; 64 × 64 matrix; 3.125 mm^2 in-plane resolution; 5 mm thickness with 0 mm skip; 30 ms echo time; 1500 ms repetition time; 90 degrees flip angle; 20 cm^2 field of view. During fMRI, only Type 0 and 2 trials (no interference and both types of interference; see Figure 1B) were employed. The task was run in a block design. Each block consisted of 24 trials of the same type. One run consisted of 8 alternating blocks, with an additional five visual fixation blocks interspersed. Data were analyzed using Brain Voyager software (Brain Innovation, Maastricht, the Netherlands). Anatomical and functional data were co-registered and transformed into common Talairach space. A general linear model was constructed using predictors modeled by convolution with a standard hemodynamic response function. Single subject repeated-measures ANOVAs were performed on a voxel-wise basis. Multiple comparisons were accounted for by using a cluster constraint with regional false positive probability $p < 10^{-4}$. This constraint required a cluster of ≥7 contiguous voxels with $p < 0.05$.

Surgical procedure

The surgical procedure was performed using standard stereotactic techniques. A Cosman-Roberts-Wells (Integra, Plainsboro, NJ) stereotactic frame was affixed to the patient under local anesthesia, and a high-resolution MRI obtained. The target for the left posterior lesion (2 cm posterior to the most anterior point of the frontal horn of the lateral ventricle, 0.7 cm lateral to midline, and 0.5 cm superior to the corpus callosum) was programmed into a neuro-navigation computer (StealthStation, Medtronic, Minneapolis, MN) and the stereotactic frame was then appropriately set. The patient was positioned semi-recumbent, the surgical area prepared, and sterile drapes applied. Local anesthetic was infiltrated, a coronal skin incision was performed, and bilateral burr holes drilled 1.5 cm lateral to midline, and 10.0 cm posterior to the nasion. A computerized microelectrode drive controlled by a neurophysiology system (Alpha Omega, Alpharetta, GA) was affixed to the frame. Following dural opening, microelectrodes were lowered using the computerized drive in increments of 0.01 mm. The position of the tip of the electrodes was also monitored in real time using the stereotactic neuronavigation system. Following microelectrode recordings, a thermocoagulation electrode with a 10 mm exposed tip (Cosman Medical, Burlington, MA) was lowered to the target. Lesions were performed by heating the electrode to 85 degrees Celsius for 60 seconds. Two more pairs of lesions were then created, each 7 mm anterior and 2 mm inferior to the previous lesion.

Microelectrode Recordings

For microelectrode recordings, an array of three tungsten microelectrodes (500-1500 kΩ; FHC, Bowdoin, ME) was attached to a motorized microdrive (Alpha Omega Engineering, Nazareth, Israel). Following routine surgical protocol, recordings were obtained from the left hemisphere. Upon reaching the cingulate cortex, microelectrodes were held in place and monitored for approximately five minutes to assess signal stability. Putative neurons were not screened for task-responsiveness. Analog data were amplified, band-pass filtered between 300 Hz and 6 kHz, sampled at 20 kHz (Alpha Omega Engineering, Nazareth, Israel), and spike-sorted (Offline Sorter, Plexon, Dallas, TX).

Post-lesion Behavior

Immediately after creation of the cingulate lesions, subjects again performed the MSIT task. These task sessions were identical in all respects to the pre-lesion sessions except that we collected only behavioral data. Four of the six patients participated in these post-lesion sessions.

Reaction Time Data Analysis

Reaction time (RT) was defined as the interval between the onset of the cue and the subject's button-press. To allow for inter-subject comparisons, we normalized subject RTs relative to their individual distributions. Normalized RTs were defined as the number of standard deviations (z-scores) above or below the bottom 10^{th} percentile of a subject's RT distribution. The choice of each subject's reference point for the normalization (bottom 10^{th} percentile vs. median or mean) is arbitrary and does not affect the result, since it simply represents a rigid translation of the normalized values. We chose the bottom 10^{th} percentile so that values were positive, to facilitate visual comparisons.

We also computed a speed of target selection (STS) as per Mansouri et al. (2007).[25] We inverted response time (defined as the interval between appearance of the cue on the screen and subject button-press) to obtain STS = 1/RT. We then divided by the mean STS across all trials in the behavioral session. In this way, STS was normalized to 1, which represented an intermediate or "average" response speed. Faster responses (*e.g.* on low-conflict trials) are reflected as relative increases in STS (*i.e.* STS > 1), whereas slower responses (*e.g.* on high-conflict trials) are attended by decrements in the STS (*i.e.* STS < 1). Use of the normalized STS, rather than raw RTs, allowed us to view data from different subjects on a common scale and to minimize between-subject differences when pooling data to calculate composite statistics.

Single-unit Data Analysis

Single units were isolated by first building a histogram of peak heights from the raw voltage tracings on each channel. We applied a minimum threshold of three standard deviations to exclude background noise. Action potentials were sorted using waveform principal component analysis. Spike clusters of putative neurons were required to separate clearly from any channel noise, to demonstrate a voltage waveform consistent with that of a cortical neuron, and to have at least 99% of action potentials separated by an inter-spike interval of 1 ms or more.

We recorded an average of 1.1 neurons per microelectrode. When a single channel captured more than one neuron cluster, we required a clear distinction between the two clusters to include either one as a single unit ($p < 0.01$, multivariate ANOVA across the first two principal components). Additionally, we required putative dACC neurons to fire at an average rate of at least 1.0 spikes/sec, to be stably active for at least 25 task trials, and to not demonstrate significant drift over the duration of the recording. We excluded single units not meeting these criteria. We did not use any multi-unit activity.

We classified neurons into three mutually exclusive categories based on the timing of their peak firing rates with respect to task events. Neurons peaking in activity prior to stimulus presentation, during the stimulus period, and after the button-push were classified as “pre-cue”, “cue”, and “feedback” neurons, respectively.

To facilitate comparisons between neurons with different firing rates, we normalized (divided) neuronal activity by the average neuronal firing rate during a 500 ms window preceding appearance of the fixation point. Population firing rates were computed by averaging these normalized neuronal responses with a 250 ms moving boxcar window.

Supplementary Material

Refer to Web version on PubMed Central for supplementary material.

Acknowledgments

This work was supported by grants from the National Science Foundation (IOB 0645886), the National Institutes of Health (NEI 1R01EY017658-01A1, NIDA 1R01NS063249, NIMH Conte Award MH086400, R25 NS065743), the Klingenstein Foundation, the Howard Hughes Medical Institute, the Sackler Scholar Programme in Psychobiology, the Centers for Disease Control (5 R01 DP000339), the Benson-Henry Institute at MGH for Mind-Body Medicine, the David Judah Fund, the McIngvale Fund, and the Center for Functional Neuroimaging Technologies (P41RR14075).

References

1. Williams ZM, Bush G, Rauch SL, Cosgrove GR, Eskandar EN. Human anterior cingulate neurons and the integration of monetary reward with motor responses. Nat Neurosci. 2004; 7:1370–1375. [PubMed: 15558064]
2. Botvinick M, Nystrom LE, Fissell K, Carter CS, Cohen JD. Conflict monitoring versus selection-for-action in anterior cingulate cortex. Nature. 1999; 402:179–181. [PubMed: 10647008]
3. Brown JW, Braver TS. Learned predictions of error likelihood in the anterior cingulate cortex. Science. 2005; 307:1118–1121. [PubMed: 15718473]
4. Gratton G, Coles MG, Donchin E. Optimizing the use of information: strategic control of activation of responses. J Exp Psychol Gen. 1992; 121:480–506. [PubMed: 1431740]
5. Hayden BY, Platt ML. Neurons in anterior cingulate cortex multiplex information about reward and action. J Neurosci. 2010; 30:3339–3346. [PubMed: 20203193]
6. Narayanan NS, Laubach M. Neuronal correlates of post-error slowing in the rat dorsomedial prefrontal cortex. J Neurophysiol. 2008; 100:520–525. [PubMed: 18480374]
7. Botvinick MM, Cohen JD, Carter CS. Conflict monitoring and anterior cingulate cortex: an update. Trends Cogn Sci. 2004; 8:539–546. [PubMed: 15556023]
8. Carter CS, van Veen V. Anterior cingulate cortex and conflict detection: an update of theory and data. Cogn Affect Behav Neurosci. 2007; 7:367–379. [PubMed: 18189010]
9. Carter CS, et al. Anterior cingulate cortex, error detection, and the online monitoring of performance. Science. 1998; 280:747–749. [PubMed: 9563953]
10. Nieuwenhuis S, Schweizer TS, Mars RB, Botvinick MM, Hajcak G. Error-likelihood prediction in the medial frontal cortex: a critical evaluation. Cereb Cortex. 2007; 17:1570–1581. [PubMed: 16956979]
11. Davis KD, Hutchison WD, Lozano AM, Tasker RR, Dostrovsky JO. Human anterior cingulate cortex neurons modulated by attention-demanding tasks. J Neurophysiol. 2000; 83:3575–3577. [PubMed: 10848573]
12. Davis KD, et al. Human anterior cingulate cortex neurons encode cognitive and emotional demands. J Neurosci. 2005; 25:8402–8406. [PubMed: 16162922]

13. Bush G, Shin LM. The Multi-Source Interference Task: an fMRI task that reliably activates the cingulo-frontal-parietal cognitive/attention network. Nat Protoc. 2006; 1:308–313. [PubMed: 17406250]
14. Bush G, Shin LM, Holmes J, Rosen BR, Vogt BA. The Multi-Source Interference Task: validation study with fMRI in individual subjects. Mol Psychiatry. 2003; 8:60–70. [PubMed: 12556909]
15. Bush G, et al. Functional magnetic resonance imaging of methylphenidate and placebo in attention-deficit/hyperactivity disorder during the multi-source interference task. Arch Gen Psychiatry. 2008; 65:102–114. [PubMed: 18180434]
16. Fellows LK, Farah MJ. Is anterior cingulate cortex necessary for cognitive control? Brain. 2005; 128:788–796. [PubMed: 15705613]
17. Kerns JG, et al. Anterior cingulate conflict monitoring and adjustments in control. Science. 2004; 303:1023–1026. [PubMed: 14963333]
18. Nakamura K, Roesch MR, Olson CR. Neuronal activity in macaque SEF and ACC during performance of tasks involving conflict. J Neurophysiol. 2005; 93:884–908. [PubMed: 15295008]
19. Holroyd CB, Coles MG. The neural basis of human error processing: reinforcement learning, dopamine, and the error-related negativity. Psychol Rev. 2002; 109:679–709. [PubMed: 12374324]
20. Botvinick MM. Conflict monitoring and decision making: reconciling two perspectives on anterior cingulate function. Cogn Affect Behav Neurosci. 2007; 7:356–366. [PubMed: 18189009]
21. Ito S, Stuphorn V, Brown JW, Schall JD. Performance monitoring by the anterior cingulate cortex during saccade countermanding. Science. 2003; 302:120–122. [PubMed: 14526085]
22. Mayr U, Awh E, Laurey P. Conflict adaptation effects in the absence of executive control. Nat Neurosci. 2003; 6:450–452. [PubMed: 12704394]
23. Ridderinkhof KR. Micro- and macro-adjustments of task set: activation and suppression in conflict tasks. Psychol Res. 2002; 66:312–323. [PubMed: 12466928]
24. Mansouri FA, Buckley MJ, Tanaka K. Mnemonic function of the dorsolateral prefrontal cortex in conflict-induced behavioral adjustment. Science. 2007; 318:987–990. [PubMed: 17962523]
25. Gehring WJ, Fencsik DE. Functions of the medial frontal cortex in the processing of conflict and errors. J Neurosci. 2001; 21:9430–9437. [PubMed: 11717376]
26. di Pellegrino G, Ciaramelli E, Ladavas E. The regulation of cognitive control following rostral anterior cingulate cortex lesion in humans. J Cogn Neurosci. 2007; 19:275–286. [PubMed: 17280516]
27. Cole MW, Yeung N, Freiwald WA, Botvinick M. Cingulate cortex: diverging data from humans and monkeys. Trends Neurosci. 2009; 32:566–574. [PubMed: 19781794]
28. Rauch SL, et al. Volume reduction in the caudate nucleus following stereotactic placement of lesions in the anterior cingulate cortex in humans: a morphometric magnetic resonance imaging study. J Neurosurg. 2000; 93:1019–1025. [PubMed: 11117844]
29. Asaad WF, Eskandar EN. A flexible software tool for temporally-precise behavioral control in Matlab. J Neurosci Methods. 2008; 174:245–258. [PubMed: 18706928]
30. Miller EK, Cohen JD. An integrative theory of prefrontal cortex function. Annu Rev Neurosci. 2001; 24:167–202. [PubMed: 11283309]

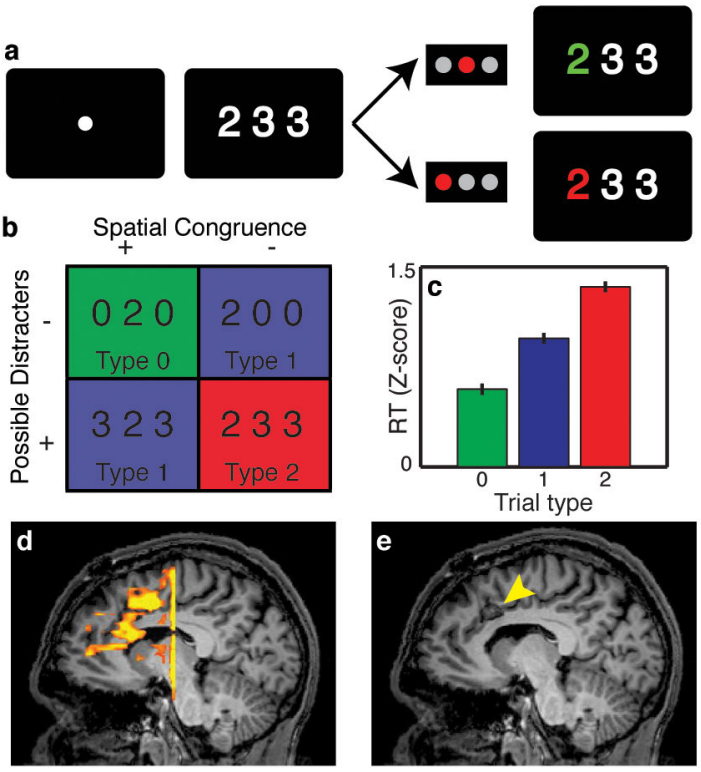

Fig. 1.

Behavioral task, functional MRI, and subject performance. (**A**) The Multi-Source Interference Task. (**B**) Four trial types are possible, based on whether there is spatial congruence between the position of the target and correct button response, and whether the distracters are possible (“1”, “2”, “3”) or impossible (“0”) button choices. (**C**) Reaction times increased with increasing cognitive interference in the cue ($p<1\times10^{-20}$, ANOVA, error bars s.e.m., n=1545). (**D**) Representative example showing increased dACC fMRI activation during high- vs. non-interference trials. (**E**) A mid-sagittal slice depicting the lesion (arrowhead), which is also the site of microelectrode recordings.

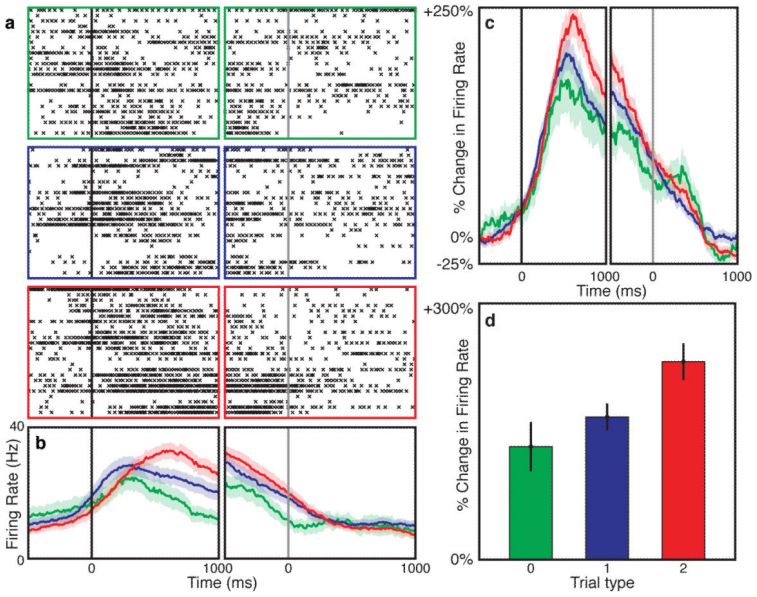

Fig. 2.

Individual and population neuronal responses. (**A**) Example neuron showing modulation of firing based on cue-related interference. Rasters for Type 0 (green), 1 (blue), and 2 (red) trials are shown aligned to the cue (black line) and choice (gray line). (**B**) Average firing rates of the same neuron. Error bars (s.e.m., n=72) are depicted with shading. Firing rates (**C**) and averaged activity within a 200 ms wide window centered 500 ms after the cue (**D**) for all cue-related neurons. Neuronal firing increased with cognitive interference (p=0.02, ANOVA), correlating with RT.

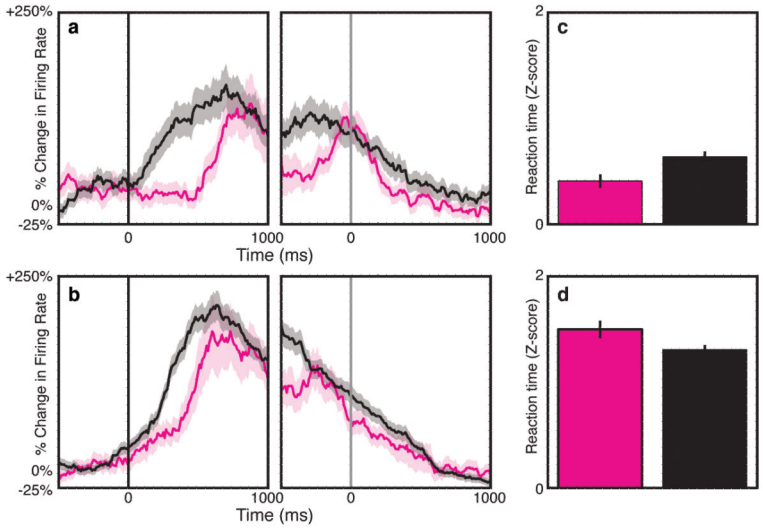

Fig. 3.

Effect of previous trial on dACC firing and reaction time. (**A**) Activity was greater for current non-interference trials immediately preceded by interference trials (1,2→0; black) than non-interference trials (0→0; purple). (**B**) Similarly, activity was greater for high interference trials preceded by interference (1,2→2; black) than non-interference trials (0→2; purple). (**C**) Reaction times for non-interference trials were shorter (p=0.008) when preceded by non-interference (0→0; purple) than interference (1,2→0; black) trials. (**D**) RTs for high interference trials were shorter (p=0.04) when preceded by interference (1,2→2; black) than non-interference (0→2; purple) trials. Shading and error bars represent s.e.m (n=816).

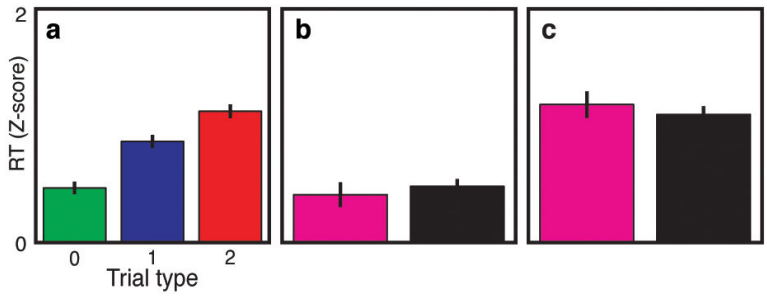

Fig. 4.

Abolition of behavioral adaptation following a targeted dACC lesion. RTs were recorded following cingulotomy, in which a stereotactic lesion was created precisely in the region of the dACC from which fMRI signals and microelectrode recordings were obtained. (**A**) RTs followed a dose-response pattern by trial type ($p<1\times10^{-12}$, ANOVA) similar to that before the lesion (Figure 1C). Error bars represent s.e.m (n=572). Behavioral adaptations (the influences of previous trial identity on current trial reaction times), however, were abolished for both **(B)** non-interference ($p=0.54$) and **(C)** high-interference ($p=0.53$) trials.